# Comparison of water-soluble and insoluble organic compositions attributing to different light absorption efficiency between residential coal and biomass burning emissions

Lu Zhang [1,2], Jin Li [1], Yaojie Li[1], Xinlei Liu [1], Zhihan Luo [1], Guofeng Shen [1,*], and Shu Tao [1,3]

1. *Laboratory for Earth Surface Process, College of Urban and Environmental Sciences, Peking University, Beijing 100871, China*

2. *Hong Kong Polytechnic University, Department of Civil & Environmental Engineering, Kowloon, Hong Kong, China*

3. *College of Environmental Science and Technology, Southern University of Science and Technology, Shenzhen 518055, China*

** Corresponding author: Dr. Guofeng Shen, Peking University, Email: gfshen12@pku.edu.cn*

**Abstract**

There are growing concerns about the climate impacts of absorbing organic carbon (also known as Brown Carbon, BrC) in the environment, yet its chemical composition and association with the light absorption capabilities remain poorly understood. This study characterized water-soluble and water-insoluble organic carbon (WSOC, WIOC) from residential solid fuel combustion at the molecular level and evaluated their quantitative relationship with mass absorption efficiency (MAE). The MAE values at λ=365 nm from biomass burning were significantly higher than those from coal combustion ($p$<0.05). Thousands of peaks were identified in the m/z range of 150-800, with the most intense ion peaks occurring between 200-500 m/z for WSOC and 600-800 m/z for WIOC, respectively. The CHO group predominated in WSOC extracts from biomass burning emissions while sulfur-containing compounds (SOCs) including CHOS and CHONS were more intense in the WIOC extracts, particularly from coal emissions. Emissions of the CHON group were positively correlated with the fuel nitrogen content (r=0.936, $p$<0.05), explaining their higher abundance in coal emissions compared to biomass. The SOCs emissions were more predominant during flaming phases, as indicated by a positive correlation with modified combustion efficiency (MCE) (r=0.750, $p$<0.05). The unique formulas of coal combustion aerosols were in the lower H/C and O/C regions with higher unsaturated compounds in the van Krevelen (VK) diagram. In WIOC extracts, coal combustion emissions contained significantly higher fractions of condensed aromatics (32-59%), compared to only 4.3-9.7% in biomass burning emissions. However, the CHOS group in biomass burning emissions was characterized by larger condensed aromatic compound fractions than those in coal combustion. The CHOS aromatic compound fractions were positively correlated with MAE values in both WSOC (r=0.714, $p$<0.05) and WIOC extracts (r=0.929, $p$<0.001), suggesting these compounds significantly contributed to MAE variabilities across different fuels.

*Keywords:* light absorption properties, atmospheric aerosols, N-containing compounds, S-containing compounds, water-soluble compounds, water-insoluble compounds.

**TOC**

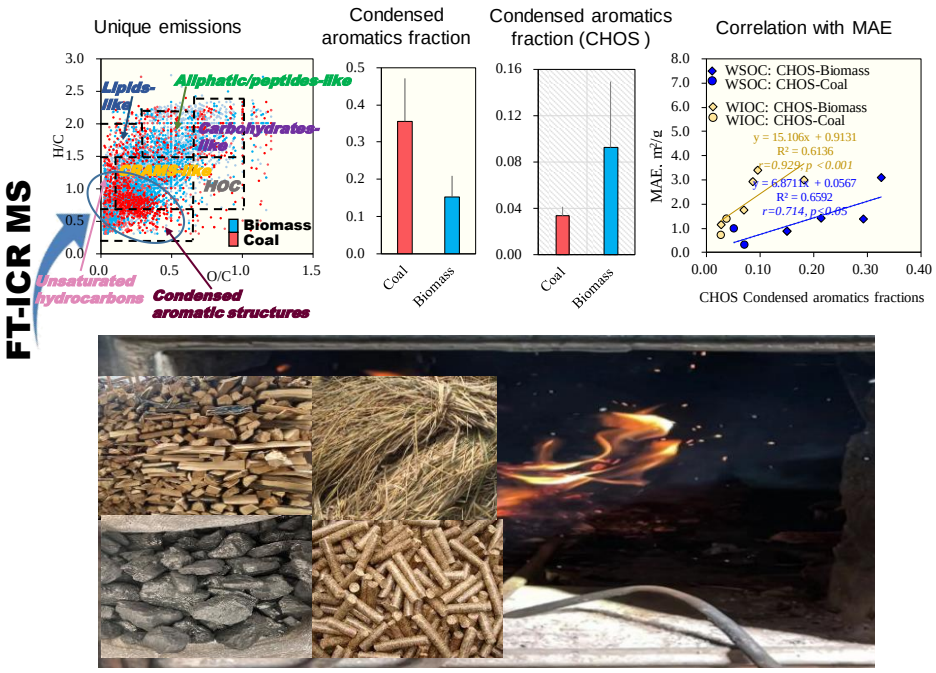


## 1. Introduction

Light-absorbing organic carbon (OC), known as Brown Carbon (BrC), attracts growing concerns due to its direct radiative impact on climate change (Laskin et al., 2015; Wang et al., 2022). The global simulations suggested that BrC may contribute nearly 20% of the surface organic aerosol (OA) burden (Jo et al., 2016), and accounted for 19% of the light absorption by anthropogenic aerosols (Feng et al., 2013). BrC originates from diverse sources, including primary emissions from coal combustion, biomass burning, and vehicular emissions (Du et al., 2014; Olson et al., 2015; Bond, 2001; Sun et al., 2017; Chen and Bond, 2010), and secondary processes like the oxidation of volatile organic compounds (Guan et al., 2020; Laskin et al., 2015). Among these sources, residential solid fuel burning produced large amounts of BrC, accounting for 74% of the total anthropogenic primary emissions (Xiong et al., 2022).

Some efforts have been made to explore the BrC physiochemical properties in residential emissions. For example, water-soluble organic carbon (WSOC) and methanol-soluble organic carbon (MSOC) were analyzed in primary emissions from combustions of crop straw, wood fuel, and some coals (Park and Yu, 2016). Available studies suggested that the optical properties of primary BrC varied significantly, influenced by numerous factors including inherent fuel properties and combustion conditions. Mass absorption efficiency (MAE) is a key parameter in assessing the direct radiative forcing of light-absorbing carbonaceous aerosols (Huo et al., 2018). It was found that water-soluble BrC derived from bituminous coals had higher MAE values than anthracites (Tang et al., 2020). However, the specific chemical components responsible for the differences in light absorption among various fuel types are not yet fully understood, especially at the molecular level. It was also reported that the mass absorption of water-insoluble organic carbon (WIOC) could be even greater than that of the water-soluble ones (Chen and Bond, 2010; Huang et al., 2018). However, there is limited information available regarding their chemical components. Given the significant variation in BrC light absorption across different fractions emitted from various fuels (Xie et al., 2017), detailed information of a comprehensive characterization, including the chemical and optical characteristics of the BrC fractions (both water-soluble and water-insoluble) from the combustion source, is needed.

This study investigated the chemical compositions and light absorption abilities of WSOC and WIOC in smoke particles generated from the burning of coals with different maturity, raw biomass fuels, and biomass pellets in traditional and improved stoves. The use of biomass pellets has been heavily promoted over the last several years to mitigate air pollutant emissions from traditional solid fuels, and emission characteristics from improved stoves could be different from traditional ones. Optical property variations were quantitatively assessed and analyzed to explore their association with chemical components. Furthermore, unique molecules and fingerprints for coal and biomass

sources were discussed, which is critical in pollution source appointment.

## 2. Materials and methods

### 2.1 Laboratory combustion emission experiment

In the present study, a total of fourteen types of coals with varying maturity degrees, five types of biomass pellets, and twelve types of raw biomass were examined using a laboratory combustion system. Two types of stoves, including a traditional stove (TS) and an improved stove (IS), were utilized for the experiments. The thirty-four fuel-stove combinations are listed in Table S1. The combustion tests were performed in a specially designed system with real-time online monitors (Thermo Scientific Inc., Bremen, Germany), which are capable of continuously measuring gaseous pollutants, including CO, $CO_2$, hydrocarbons (HC), and nitrogen oxide ($NO_X$ including NO and $NO_2$). $PM_{2.5}$ (particles with aerodynamic diameters ≤2.5 μm) was collected at a flow rate of 16.7 L/min with the quartz filters. Fuel properties including moisture ($M_{ad}$, %), volatile matter content ($V_{daf}$, %), ash content ($A_{ad}$, %), lower heating value (LHV, MJ/kg), and contents of carbon (C, %), hydrogen (H, %), nitrogen (N, %), and sulfur (S, %) are tested, and listed in Table S1. Details of stove construction and combustion processes were available in Zhang et al., (2022).

Modified combustion efficiency (MCE) was calculated by integrating the incremental concentrations of $CO_2$ and CO as:

$$\mathrm{MCE} = \frac{\mathrm{CO_2}}{\mathrm{CO_2 + CO}}$$

where $CO_2$ and CO represent the excess molar mixing ratios of $CO_2$ and CO, respectively (Pokhrel et al., 2016). The MCE values indicate different phases of combustion: approximately 1 during flaming, and between 0.7-0.9 during smoldering (Yokelson et al., 1997)

## 2.2 Bulk carbon and UV-vis absorption spectra

For each sample, a 4.9 $cm^2$ filter was extracted ultrasonically with 10 mL Milli-Q water (18.2 MΩ) for 30 min, and then the supernatant was separated. The extraction process was repeated twice, and the extracts were combined. The water extract was then filtered via a 0.22 μm polytetrafluoroethylene (PTFE) filter to obtain WSOC. Due to the inefficiency of water in extracting BrC, the insoluble PM components remaining on the sample filter were freeze-dried and subjected to methanol extraction through sonication. The resulting extract was then filtered using a PTFE filter, yielding a water-insoluble fraction referred to as WIOC in the following text. The carbon content of WSOC was analyzed with a total organic carbon (TOC) analyzer (TOC-Lcph/cpn, SHIMADZU, Japan), and the WIOC was determined by subtracting WSOC from the total OC loaded on the same 4.9 $cm^2$ area, given that the methanol extraction efficiency for all combustion samples was up to 90% (Zhang et al., 2022). The element carbon (EC) and OC were measured using a thermal-optical analyzer (Sunset OC/EC analyzer) with an interagency monitoring of protected visual environments (IMPROVE) program.

The light absorption spectra of the water and methanol extracts were measured between 200 nm and 600 nm by UV–vis spectrophotometer (UV-2600, Shimadzu, Japan) at a step size of 1 nm. MAE values of WSOC and WIOC at the wavelength of λ ($MAE_{\lambda, WSOC}$; $MAE_{\lambda, WIOC}$) were calculated as following equation (Li et al., 2019):

$$MAE_{\lambda, WSOC}=A_{\lambda, WSOC}\times\ln(10)/(C_{WSOC}\times L);\ MAE_{\lambda, WIOC}=A_{\lambda, WIOC}\times\ln(10)/(C_{WIOC}\times L)$$

where $A_{\lambda, WSOC}$ and $A_{\lambda, WIOC}$ is the light absorption value of WSOC extract and WIOC extract at a wavelength of λ, respectively; C is the concentration of WSOC (or WIOC), and L is the optical path length, which is 0.01 m in this study. It is important to note that the reported light absorption of WIOC in this study was underestimated, while such underestimation is insignificant due to the high extraction efficiency. In this study, the MAE values of extractable OC at λ of 365 nm ($MAE_{365,}$

$_{WSOC}$ and $MAE_{365, WIOC}$) were discussed.

Absorption Ångström exponent (AAE) values were determined based on the following equation (Li et al., 2019; Li et al., 2020):

$$A_\lambda = K_\lambda^{-AAE}$$

where K is a constant and AAE is obtained through the linear regression of lg ($A_\lambda$) against lg λ (Fig S1). A wavelength of 300-400 nm is chosen according to the published literature (Yue et al., 2022), and the goodness of fit for all the samples in this study is greater than an $r^2$ of 0.99.

## 2.3 Molecular composition analysis

For further molecular composition analysis, the WSOC and WIOC extracts from seven selected source samples were subjected to Fourier-transform ion cyclotron resonance mass spectrometry (FT-ICR MS) coupled with electrospray ionization (ESI). These samples included two types of coals (high volatile bituminous coal, HVB; medium volatile bituminous coal, MVB) combusted in TS, two types of raw biomass (rice straw and pine wood) combusted in TS, pine wood combusted in IS, and two types of biomass pellets (crop straw pellet and pine wood pellet) combusted in IS as noted in SI. FT-ICR MS has been successfully applied for the molecular-level characterization of compounds (Bianco et al., 2018) due to its ultrahigh resolution and mass accuracy. ESI is well-adopted to characterize soluble aerosols, especially for the detection of polar, hydrophilic molecules like humic-like substances (HULIS)-type compounds (Wozniak et al., 2008), because it is a “soft” ionization technique generating minimal analyte fragments, and thus can detect intact molecules of compounds. Therefore, the negative ESI-FT-ICR was applied here to determine the molecular compositions of WSOC and WIOC from combustion samples from different solid fuels. The methanol extracts were evaporated to dryness under a gentle stream of nitrogen and then dissolved with Milli-Q water. The WSOC and water-reconstituted WIOC were submitted to solid-phase

extraction (SPE) using Bond Elut PPL (500 mg, 6 mL, Agilent, U.S.A.). Before the extraction, the PPL cartridges were sequentially conditioned with 12 mL methanol and 12 mL Milli-Q water containing 0.05% hydrochloric acid (HCl). The extract was adjusted to pH=2 using HCl to remove inorganic ions and was then loaded onto the PPL cartridges at a rate of 5 mL/min. Cartridges were washed with 18 mL Milli-Q water containing 0.05% HCL to remove salt and then dried under pure nitrogen. Analytes were eluted with 12 mL methanol, and the combined eluates were concentrated to 1 mL. Then the molecular characterization was conducted using a 15T SolariX XR FT-ICR MS (Bruker Daltonik GmbH, Bremen, Germany) in the negative ESI mode. The capillary inlet voltage was set at -4.0 kV and ion accumulation time was set to 0.06 S. There were 300 continuous 4 M data FT-ICR transients added to improve the signal-to-noise ratio. The FT-ICR MS was calibrated with 10 mmol/L sodium formate in advance, and internal standard calibration with soluble organic matter (known molecular formula) was performed after the test. Finally, <1 ppm absolute mass error was achieved. Data processing details are described in the Supporting Information (SI).

## 3. Result and discussion

### 3.1 Optical characteristics of WSOC and WIOC

MAE is an important parameter reflecting the light absorption capability of the carbonaceous aerosols. The $MAE_{365, WSOC}$ of aerosols from residential sources in this study ranged from 0.21 to 3.1 $m^2/g$ with an average of 1.3±0.7 $m^2/g$. MAE values of extractable OC in this study were lower than that of 11.3 $m^2/g$ for pure BC aerosols (Bond and Bergstrom, 2006) and also lower than that from the filter-based MAE values of OC of 0.16-13 $m^2/g$ from residential sources (Zhang et al., 2021b). A significant difference ($p$<0.05) of $MAE_{365, WSOC}$ was observed among the different fuels (Fig.1). The $MAE_{365, WSOC}$ of raw biomass combustion derived aerosols averaged at 1.7±0.8 $m^2/g$, which was significantly higher ($p$<0.05) than those from coal smoke (0.93±0.44 $m^2/g$) and biomass

pellet smoke (1.2±0.6 $m^2/g$). The $MAE_{365, WIOC}$ ranged from 0.49 to 6.6 $m^2/g$ with an average of 2.0±1.3 $m^2/g$. The absorption capability was higher for the WIOC extract than the WSOC extract. This is thought to be associated with distinct chemical compositions of light-absorbing organics. It was noted that the WIOC had higher MAE values compared to the WSOC, which may be explained by the more hydrophobic PAHs and quinones (Chen and Bond, 2010). The difference in $MAE_{365, WIOC}$ among the different fuels was also statistically significant ($p$<0.05), as the value obtained from raw biomass burning (2.8±1.4 $m^2/g$) was significantly higher than that from coal combustion (1.2±0.6 $m^2/g$). It was suggested that the MAE values of soluble OC including WSOC and WIOC were dependent on the chemical composition of OC, that is, the chemical structure of the light-absorbing chromophores and the ratio of non-light-absorbing organics to the chromophore components (Cao et al., 2021). The higher MAE values of raw biomass combustion-derived aerosols might be caused by the stronger light absorption capability of chromophores or a higher ratio of chromophores. Our result was comparable to the published data, for example, the $MAE_{365, WSOC}$ was reported to average at 1.37±0.23 $m^2/g$ for biomass burning emissions (Park and Yu, 2016). The correlation of MAE with the MCE was investigated. The variability in MAE values, for both WSOC and WIOC, was observed to be negatively correlated with the MCE (or temperature as MCE was found to be positively correlated with the measured temperature in emission exhausts) when pooling all data together as seen in Fig. 1C and 1D. However, within each fuel group, there was no statistically significant correlation between the MAE and MCE values (Fig. S2). Some previous studies found that OC from wood pyrolysis under higher temperature conditions had stronger absorption capability (Chen and Bond, 2010; Saleh et al., 2014), but relatively higher mass absorption coefficient (MAC) values were also reported for the organic aerosol from wood combustion under the 150°C<T<250°C compared to emissions at a lower (T<150°C) or higher (250°C<T<380°C) temperature condition (Rathod et al., 2017). Chen et al., (2010) reported that that

absorption per mass (α/ρ) of methanol extracts increased with increased wood pyrolysis temperature, but such increase was nonlinear and varied in burning emissions of different fuel types or wood with different sizes. Therefore, the negative correlations between MAE and MCE values when pooling all data together in Fig. 1 were from distinct absorption properties of emissions from different fuel types, rather than conditions like combustion temperature.

The AAE which indicates the wavelength dependence of light absorption is also an important parameter in climate models. The calculated AAE in the WSOC extract ($AAE_{WSOC}$) ranged from 3.8 to 11 with an average of 6.9±1.5, and the difference in $AAE_{WSOC}$ values among the different fuels was statistically significant ($p<0.05$) (Fig.1). The highest values were observed for the aerosols from raw biomass combustion of 7.5±1.4, followed by coal smoke of 6.7±1.5 and biomass pellet smoke of 5.6±1.2. The AAE values in the WIOC extract ($AAE_{WIOC}$) were slightly lower than $AAE_{WSOC}$, which ranged from 4.2 to 6.5 with an average of 5.5±0.5. The differences in $AAE_{WIOC}$ values among the different fuels were statistically insignificant ($p>0.05$), with averaged values of 5.8±0.3 for coal smoke, 5.1±0.9 for biomass pellet smoke, and 5.2±0.4 for raw biomass smoke. There was a weak positive correlation of $AAE_{WIOC}$ between the MCE values ($p<0.05$). The filter-based analysis also showed that AAE values were positively correlated with MCE values, indicating that more BrC were produced under the smoldering phase compared with BC (Zhang et al., 2020). This study suggested that BrC in WIOC extract was apt to be generated during the smoldering phase in comparison with the non-light-absorbing OC. The AAE values in soluble OC in this study were higher than 4 for all samples, confirming the contribution of BrC to aerosol absorptivity from source emission. The result of this study was comparable to the published literature. For example, it was reported that the $AAE_{WSOC}$ was in the range of 8.6-15 from coal combustion-derived aerosols (Song et al., 2019), and 6.2-9.3 from biomass smoke (Park and Yu, 2016). The $AAE_{WIOC}$ from wintertime

211 urban aerosols were 5.4 ± 0.2 in Xi'an and 5.7 ± 0.2 in Beijing (Huang et al., 2020).

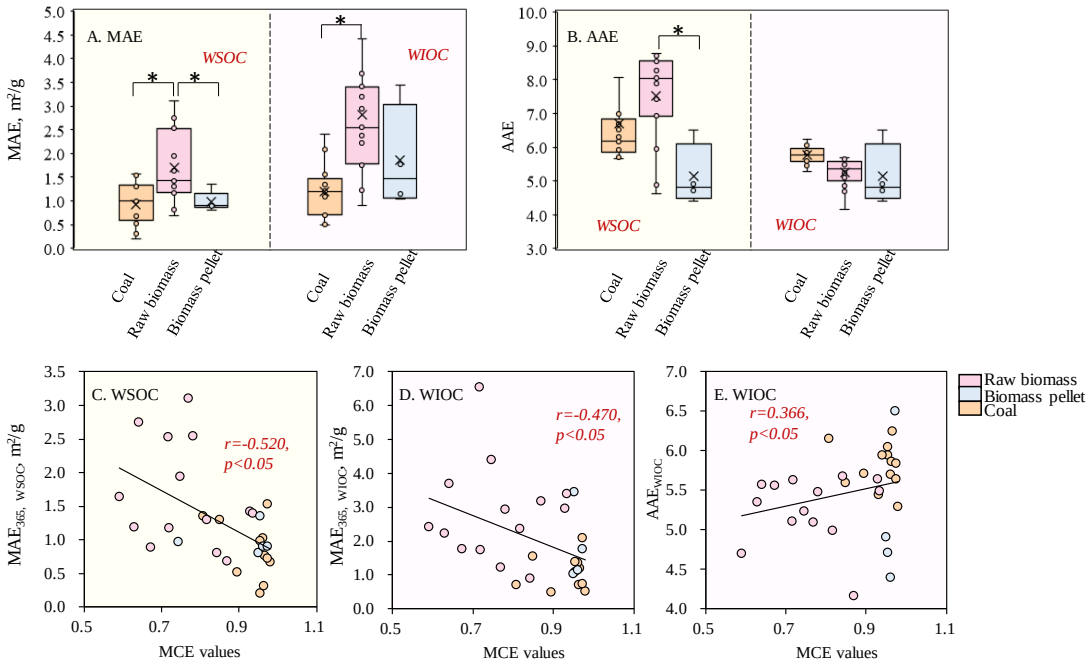


212 **Fig. 1** MAE values at λ=365 nm (A) and AAE values (B) from the source samples (* represents
213 $p$<0.05); Correlation between the MCE values with $MAE_{365, WSOC}$ values (C), $MAE_{365, WIOC}$ values
214 (D), and $AAE_{WIOC}$ values (E).

215 3.2 Molecular characteristics of WSOC and WIOC

216 The ESI-FT-ICR mass spectra of WSOC and WIOC samples are presented in Fig. 2. Thousands
217 of peaks were identified in the m/z range of 150-800, indicating a complex chemical composition
218 of aerosols from residential sources. Formulas detected in the raw biomass burning aerosols were
219 significantly higher than those in biomass pellet and coal smoke (Fig. S3), which indicated a higher
220 chemical complexity of raw biomass emissions. In addition, the combustion of pine wood in the
221 improved stove generated fewer compounds, which was 93% of the peaks identified in the
222 traditional stove (Table S2). The likely less complexity might be due to higher combustion
223 efficiencies and temperature in the improved stove. Generally, higher levels of organic aerosol mass
224 would be emitted during less efficient fuel burning, resulting from prolonged smoldering or

incomplete burning (Holder et al., 2016). Our results suggested that corresponding higher chemical complexity was also produced during the incomplete combustion in the traditional stove. The most intense ion peaks were distributed in the 200-500 m/z for WSOC, accounting for 58-86% of the total intensity. Similar results were also found in residential coal combustion (Song et al., 2019), biomass burning (Song et al., 2018), and ambient aerosols (Wozniak et al., 2008).

The mass spectra of WIOC are different from the WSOC, especially in aerosol emitted from coal combustion (Fig. 2). WIOC contained more molecules with larger m/z values of 600-800 in range, which indicated that WIOC extract had more compounds with higher molecular weight (MW) than the WSOC extract. According to the molecular formulas and the intensity of each negative ion, the average molecular formulas for the WSOC were obtained with C atom from 20 to 24, H (21-29), N (0.32-0.75), O (5.6-7.0), and S (0.28-0.51) in the WSOC extract. All aerosols from biomass burning, either raw or pelletized ones, had higher relative O atom contents than coal smoke, indicating a higher oxidation degree of biomass emissions. For the WIOC, the average molecular formulas were assigned with 27-33 C, 26-35 H, 0.67-1.2 N, 6.6-11 O, and 0.34-0.92 S. The coal combustion-derived aerosols had more C, N, and S atoms, but less H atom, compared with raw biomass. The combustion of biomass pellets is also assigned with relatively higher S elements. In addition, the WIOC fraction had a higher relative atom content than the corresponding formulas of WSOC from the same source aerosol samples. These results indicated that in addition to the fuel type, extraction solvent also had an important impact on the elemental composition of extractable BrC.


245 **Fig. 2** Negative ESI FT-ICR mass spectra of WSOC (A-G) and WIOC (A'-G') from the seven
246 aerosol samples, TS represents combustion in the traditional stove and IS represents combustion in
247 the improved stove. Different formula groups were color-coded. The pie charts showed the relative
248 intensities of different formula groups.

249 Molecular formulas identified by the FT-ICR-MS can be classified into 4 groups according to
250 the elemental composition, including CHO (containing only C, H, O), CHON (hereafter similarly),
251 CHOS, and CHONS. CHO was the most abundant group in the WSOC. The CHO group contributed
252 51-67% to the total intensity of aerosols from raw biomass burning, which were significantly higher
253 than those from biomass pellets (29-39%) and coal smoke (30-40%). The CHO compounds with
254 oxygen-containing functional groups (e.g., hydroxyl, carbonyl, carboxyl, or esters) have been
255 widely identified in both ambient aerosols (Jiang et al., 2021; Mo et al., 2022) and some source

samples (Tang et al., 2020). These compounds contributed a broad range of proportions, from 43% to 69% in residential biomass burning smoke (Tang et al., 2020), 9.7-48% in coal smoke (Song et al., 2019), and 20-39% in ambient aerosols (He et al., 2023) for the WSOC extract, which were comparable to ours. CHON compounds were also an important component in the aerosols, accounting for 29-36% of coal smoke, which was significantly higher than biomass burning smoke of 11-28%. One previous study reported that CHON species were more abundant in biomass burning smoke rather than in coal combustion ones (Song et al., 2018). This high fraction of CHON compounds in coal smoke might be caused by the higher nitrogen content of coals as seen in Table S1. A strongly significantly positive correlation was found between the fuel nitrogen content and CHON species percentage ($r=0.936$, $p<0.05$) (Fig. 3). Such dependence was also found in the emission factors (EFs) of $NO_X$ on fuel nitrogen content in our result (Fig. S4), as well as NOx, HCN, and $NH_3$ emissions reported by published literature (Hansson et al., 2004). Sulfur-containing compounds (SOCs; including CHOS and CHONS) abundance was lower than CHO and CHON group, accounting for only 22-42% (13–30% for CHOS and 7.9–28% for CHONS, respectively). The fractions of SOCs in the aerosols from coal combustion (25-42%) and biomass pellet burning (~42%) were comparable but significantly higher than those from raw biomass (22-31%). The abundance of SOCs was not statistically correlated with fuel S content in the present study for pooled data. However, when fuel subgroups were considered, fuels (coal or raw biomass) with higher sulfur content had higher SOCs levels. Also, higher SOCs emission was found for pine wood combusted in the improved stove which have higher combustion efficiency than that in the traditional stove. These results suggested that except for fuel sulfur content, the fuel type and combustion efficiency would also influence the SOCs emissions.

In the WIOC, the intensities of these four groups among different source samples were different from those in the WSOC. The CHO group accounted for 27-45% in raw biomass burning aerosols,

22-24% in biomass pellet smokes, and 13-22% of coal smokes. On the contrary, the SOCs abundance was significantly higher in WIOC, especially for the coals, accounting for 58% for HVB and 52% for MVB. A significantly positive correlation between the MCE values and SOCs abundance in the WIOC extract was found (r=0.750, $p$<0.05) (Fig. 3), while no clear association between fuel sulfur content and SOCs emissions was observed in the WIOC. Combining the result from the WSOC extract, the strong dependence of SOCs emissions on the combustion conditions was expected, while the fuel sulfur content had a slight influence. Notably, the SOCs abundance in aerosols from coal combustion was greatly higher than that in ambient aerosols (Lin et al., 2012), indicating that residential non-desulfurized coal combustion might be an important emitter of SOCs in atmospheric samples. The CHON group emissions were determined mainly by the fuel nitrogen content, while SOCs emissions were strongly related to the combustion conditions (e.g., flaming phase). It should be noted that the results of our analysis based on the current data without isotopic internal standard used were semi-quantitative, some uncertainties must be addressed.

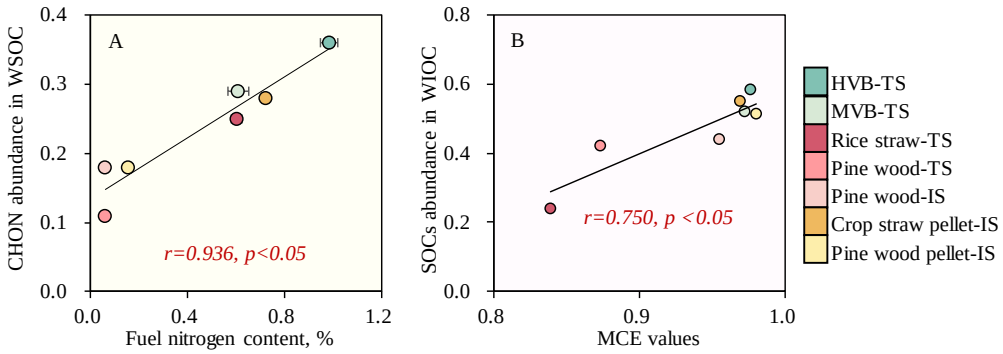


**Fig. 3** Correlation between fuel nitrogen contents and abundances of CHON in WSOC (A), and the correlation between MCE values and the abundances of SOCs in WIOC (B). TS represents combustion in the traditional stove and IS represents combustion in the improved stove.

3.3 Detailed CHO/CHON/CHOS/CHONS group differences across fuel types

Van Krevelen (VK) diagrams which can provide a visual interpretation of complex mass spectra can qualitatively identify chemical composition profiles in mixtures (Lv et al., 2016). The

299 classification criteria of the VK diagram are provided in Table S3 (Patriarca et al., 2018; Tang et al.,
300 2020). Fig. S5 and S6 show the VK diagrams of WSOC and WIOC. In both WSOC and WSOC
301 extract, the carboxylic-rich alicyclic molecules (CRAMs-like) were the most abundant component,
302 contributing to 53-69% in the WSOC extract and 37-56% in the WIOC extract, respectively. The
303 condensed aromatics were also an important component in source samples, accounting for 7.3-13%
304 in the WSOC, and for a higher proportion of 8.6-44% in the WIOC. This observation could be
305 attributed to the hydrophobic property of condensed aromatic hydrocarbons, leading to a lower
306 proportion in the highly polar WSOC. Among the identified formulas, 7.0-13% of total intensity in
307 the WSOC and 3.6-17% in the WIOC were the aliphatic/peptide-like compounds. Such fractions
308 were comparable to unsaturated hydrocarbons with percentages of 3.9-15% in the WSOC and 2.0-
309 11% in the WIOC. The compounds including lipids-like species and highly oxygenated compounds
310 (HOC) were in a relatively lower abundance, with less than 10% each in the source samples. The
311 different fuels showed varied chemical composition characteristics. Coal combustion aerosols had
312 lower H/C ratios than those in biomass burning aerosols, indicating higher unsaturated degrees
313 (Table S2). As indicated by the VK diagrams, the coal combustion produced a notable number of
314 condensed aromatics, contributing to 27%-44% of the WIOC, which was significantly higher than
315 8.6-21% in biomass burning emissions. The modified aromaticity index ($AI_{mod,w}$) which is a
316 measure of aromatic and condensed aromatic structure fractions, and the double bonds equivalent
317 (DBE) values which are used as a measure of the unsaturated level in a molecule were all higher for
318 coal emissions compared to the biomass emissions.

319 Distinct compound profiles being identified by the VK diagram classification criteria are
320 consistent with discrepancies in the four groups (CHO/CHON/CHOS/CHONS). For the CHO group,
321 the most intense compounds were CARMs compounds with fractions of 69-84% in the WSOC
322 extract and higher fractions of 51-80% in the WIOC extract. It was observed that raw biomass would

emit slightly more CRAMs (76-84% in the WSOC and 61-80% in the WIOC) than coal (69-73% in the WSOC and 62-69% in the WIOC) and biomass pellet (70-75% in the WSOC and 51-56% in the WIOC) combustion. The condensed aromatic compound was also a crucial component, accounting for 13-20% of the WSOC and 19-27% of the WIOC from coal emissions. These fractions were significantly higher than those found in raw biomass (4.5-10% in the WSOC, 7.9-10% in the WIOC) and biomass pellet (3.8-5.4% in the WSOC, and 11% in the WIOC) (Fig. 4). The other components accounted for a small (less than 10% each) of the total CHO intensity.

It was reported that the CHON compounds with O/N≥3 might be the organonitrates candidate and nitro-substituted compounds, attributing to the allocation of one nitro ($NO_2$) or nitrooxy ($ONO_2$) group (Bianco et al., 2018). In this study, the relative content of $CHON_{O/N\geq3}$ compounds (concerning the overall CHON) in the biomass (raw and pellet ones) ranged between 71-82% and 85-91% for the WSOC and WIOC, which is distinctly lower than those found in coal smokes (86-90% for the WSOC, and 86-95% for the WIOC) (Table S4). Moreover, the $AI_{mod,w}$ values for CHON compounds from coal combustion were higher than the biomass smokes for both WSOC and WIOC, as indicated by Table S2. It can thus be concluded that more CHON compounds with low aromaticity and a large amount of oxidized nitrogen functional groups were formed during the combustion of biomass fuels. Coal combustion emissions had more intense condensed aromatic compounds with a percentage of 45-50% for the CHON group, which were significantly higher than those from raw biomass (4.5-37%) and biomass pellet burning (14-30%). This result confirmed the conclusion that the CHON compounds produced from the combustion of coals were characterized by a relatively high aromaticity and a low degree of oxidation.

The O-rich CHOS fraction (O/S≥4) accounted for 42-71% (concerning the overall CHON group) in the WSOC and 45-95% in the WIOC. O-rich CHOS fraction (O/S≥4) content from coal

(66-70% in the WSOC, and 78-98% in the WIOC) and biomass pellet (67-71% in the WSOC, 76-87% in the WIOC) were relatively higher than the raw biomass smoke (42-56% in the WSOC, and 32-57% in the WIOC), suggesting that most of the CHOS compounds in coal and pellet smoke can be potentially assigned with more bearing sulfate ($-OSO_3H$) or sulfonate ($-SO_3$) groups. Different from CHO and CHON groups, it was found that the CHOS group in the biomass burning aerosols had a much more intense condensed aromatic structure with a percentage of 14-33% in the WSOC and 2.5-19% in the WIOC, especially for raw biomass (WSOC: 22-33%, WIOC:8.5-19%) than coal combustion (WSOC: 4.9-7.0%, WIOC: 2.5-7.0%). For the CHOS group in the WIOC extract, the unsaturated hydrocarbons were also an important component, accounting for 12-29% of raw biomass burning emissions, which were significantly higher than those in biomass pellet (6.9-11%) and coal (1.5-13%). These results indicated biomass burning emissions were characterized by higher unsaturation levels and aromaticity for the CHOS group than coal combustion.

Nearly 34-85% of CHONS formulas have many O atoms (≥7), indicating the existence of the $-NO_3$ group (Table S4). These CHONS compounds are probably nitrooxy-organosulfates (Song et al., 2019). The remaining compounds (15-66%) of the CHONS group had less than 7 atoms, implying that large amounts of CHONS compounds were assigned with reduced N (e.g., amide and nitrile, and heterocyclic aromatics). The condensed aromatic compounds identified by the VK diagram in the WIOC from coal combustion accounted for 22-64%, which was relatively higher than those from biomass burning (14-31%), indicating a higher degree of aromaticity. This was consistent with the difference observed in the $AI_{mod,w}$ values as seen in Table S2. The $AI_{mod,w}$ of WIOC in coal emissions were 0.38 for HVB and 0.60 for MVB, and the values were higher than the raw biomass (0.32-0.38) and biomass pellet (0.35-0.36), confirming a higher aromatic compounds content of coal smoke sample than biomass for CHONS group.

Therefore, the CHO, CHON, and CHONS groups generated from coal combustion were characterized by high unsaturated levels with more aromatic species, while CHOS groups had higher aromaticity degrees in biomass smoke aerosols. Aromatic compounds might be the strong BrC chromophores contributing to light absorption (Song et al., 2019). The difference in MAE between coal and biomass emissions and its association with the chemical components will be discussed in detail in section 3.5.

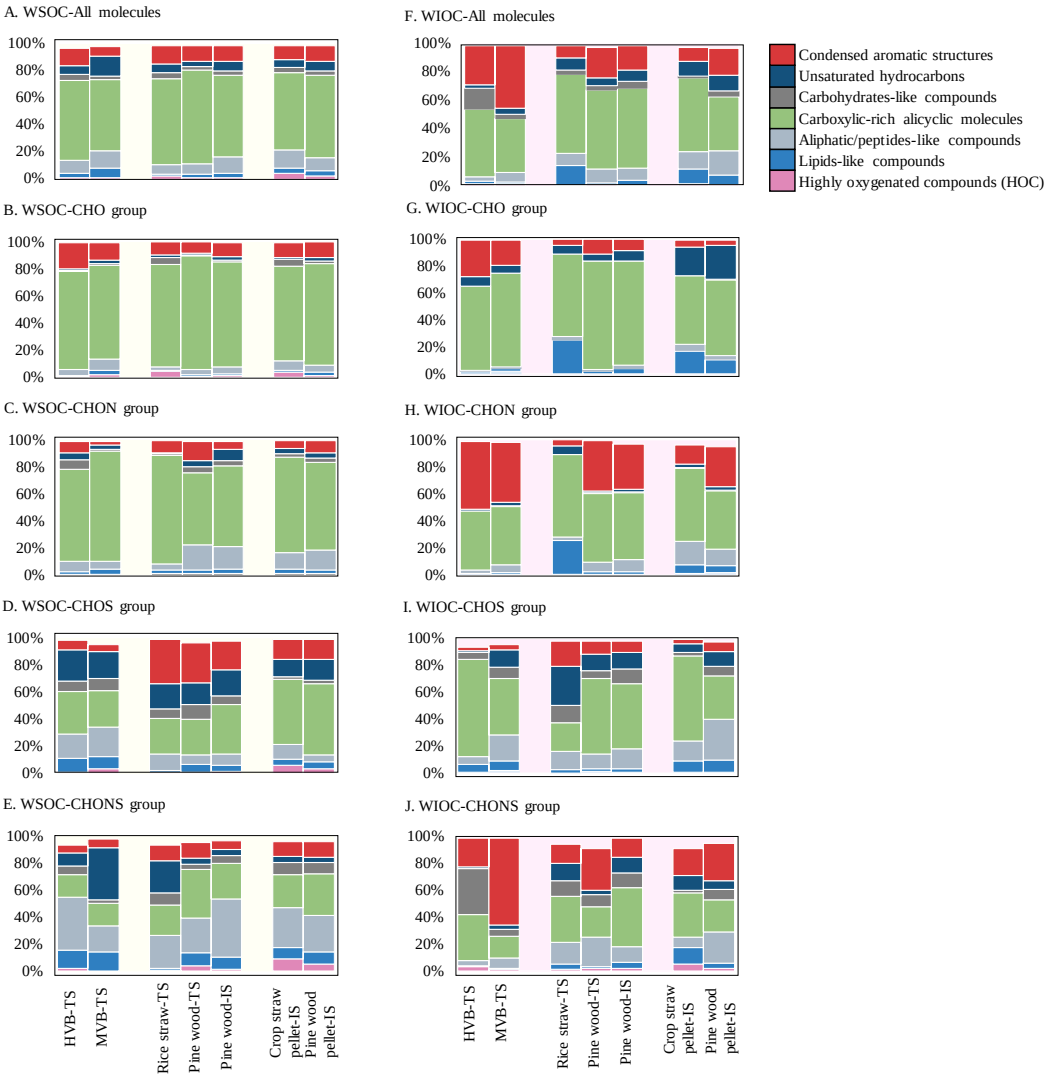


**Fig. 4** Each component abundance identified by VK diagram of WSOC (A: all molecules, B: CHO group, C: CHON group, D: CHOS group, E: CHONS group) and WIOC (F: all molecules, G: CHO group, H: CHON group, I: CHOS group, J: CHONS group), the classification criteria was provided in the Table S3.

### 3.4 Likely unique molecules of biomass and coal combustion

The unique molecules may be inferred from the Venn diagram of formulas as shown in Fig. S7. Among the observed compounds, 3039 and 1624 unique molecular formulas were detected in the combustion of rice straw and pine wood in the traditional stove in the WSOC fractions, which was significantly higher than those found in biomass pellet-improve stove (638-696) and coal-traditional stove (570-734). This suggested a notable difference between the emissions from raw biomass and coal, even when using the same stove. Interestingly, fewer unique peaks were observed for pine wood-improved stoves (533), indicating that using an improved stove for raw biomass could narrow the difference between coal and biomass emissions. A similar trend was also found in the WIOC fractions (Fig. S7). The CHONS group accounted for a significant portion of unique formulas in source samples, particularly in coal smokes, representing 51-52% in WSOC and 51-69% in WIOC extract. The important role of the CHONS group in unique emissions from coal combustion was also noted by Tang et al., (2020), who reported that CHO and CHON were the main components of unique molecular formulas of raw biomass burning emissions among the raw biomass burning, coal combustion and vehicle emissions, representing 88%-93%. This fraction was higher than our result of 33-77% in raw biomass and only 26-27% in biomass pellet. The distribution of the unique molecules further indicated substantial discrepancies among the fuels. Unique molecules in coal combustion-derived aerosols were in the region with lower H/C and O/C values compared with all other samples (Fig. 5) in both WSOC and WIOC extract, indicating a higher degree of unsaturation and lower level of oxidation. For example, it was observed that specific emissions from coal combustion were mainly composed of condensed aromatics (32-59%), followed by CRAMs compounds (23-39%) in WIOC extract. However, only 4.3-9.7% condensed aromatics of the total unique emissions were observed for biomass burning, with CRAMs being the main component (39-65%). As for different groups of CHO/CHON/ CHONS, the condensed aromatic compound contents

for all three groups in coal smoke aerosol (unique detected ones) were relatively higher than biomass. While CHOS group showed a different trend in that condensed aromatic compound contents of biomass smoke (unique detected ones) were relatively higher than coal smoke in WSOC extract and comparable to coal smoke in WIOC extract. This finding highlighted the CHOS group's importance in distinguishing the aerosols from the combustion of coals or biomass, helping conduct the source apportionment of aerosols. Additionally, compared with the pine wood-improved stove emissions, most unique molecules in aerosol from pine wood-traditional stove combustion were in the region with lower H/C and O/C ratios (Fig. 5), which were identified mainly as CRAMs compounds. The emissions from the improved stove were distributed in a wider range with fewer CRAMs compounds and more aliphatic/peptides-like compounds observed. Unique molecules from biomass pellets combusted in the improved stove distributed in the upper region of the VK diagram with higher H/C values in WIOC extract, which indicated a lower unsaturated degree (Fig. S8).

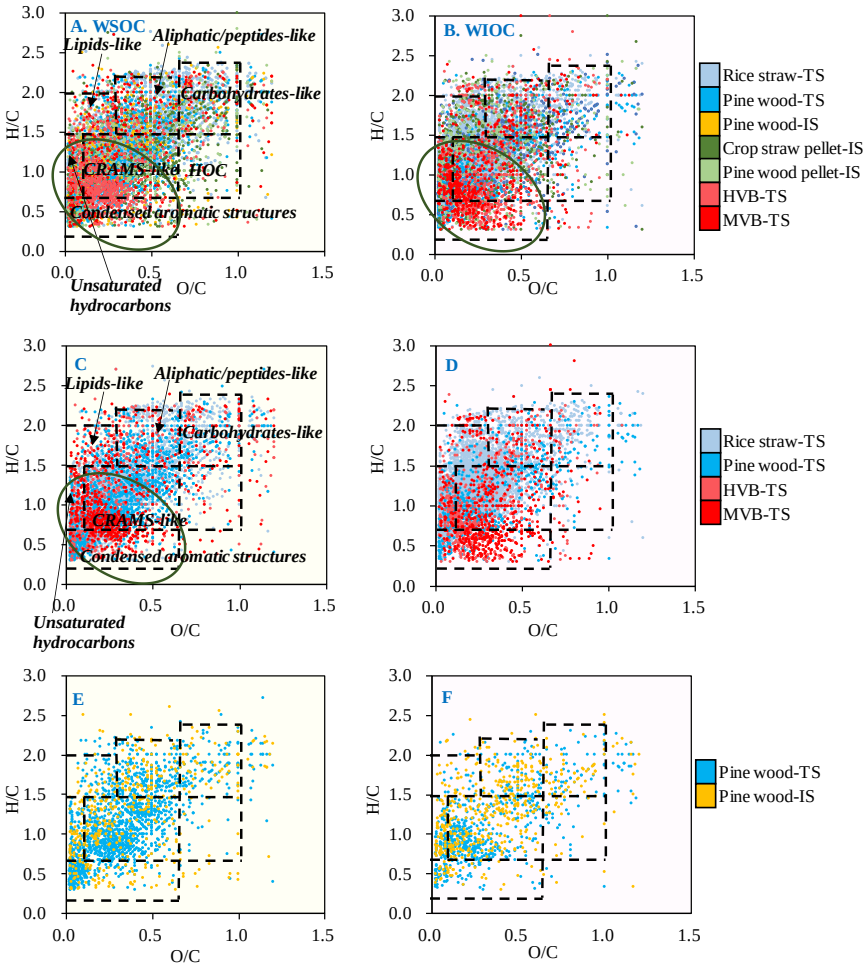


**Fig. 5** Van Krevelen diagrams of WSOC (left) and WIOC (right) from the source samples, TS represents combustion in the traditional stove and IS represents combustion in the improved stove. Different color indicates unique formulas detected in each sample of solid fuel combustion.

A total of 484 molecular formulas were detected simultaneously in the seven aerosol samples in the WSOC extract and 306 in the WIOC extract. Among these commonly detected molecules, most of which were CHO compounds with the molecular numbers accounting for 60% and 73% in the WSOC and WIOC, respectively. CHON accounted for 31% of WSOC and 19% of WIOC, while SOCs only occupied about 10%. As seen in Fig. S9, these CHO compounds were mainly composed of CRAMs-like compounds and several lipids-like and aliphatic/peptides-like compounds. Moreover, these compounds were relatively small molecular compounds assigned with 8-28 C atoms and 2-12 O atoms with DBE values of 2-17 for the WSOC extract. The relatively more C

atom assigned with larger DBE values was observed for the CHO compounds in WIOC, which could be partially explained by that the overall CHO compounds in the WIOC extract had larger MW values with a high degree of unsaturation. In total, the CHON compounds were also CRAMs-like compounds, and almost none compounds were expected to be aromatics. CHOS and CHONS species had much fewer formulas, especially for CHONS, only accounting for 1.0% of the commonly detected molecules in the WIOC. The unsaturated levels of commonly detected molecules in all seven source samples were relatively low. For example, the condensed aromatic compounds accounted for 6.5-9.3% and 3.3-4.1% of the total intensity for coal smoke and biomass smoke in the WSOC, respectively, as well as 0.38-8.3% and 18-21% in the WIOC extract. Different from the CHO, CHON, and CHONS groups, high percentages of condensed aromatic compounds were found in the CHOS group (commonly detected ones) from raw biomass burning aerosols with a range of 6.6-51% in the WSOC and 12-46% in the WIOC extract. These fractions were significantly higher than those from coal smokes of 4.1-4.9% in the WSOC and 8.8-25% in the WIOC extract. Combining the finding that the CHOS group in biomass smokes had a higher aromaticity degree in both WSOC and WIOC extract. However, the unique molecules in WIOC extract did not follow this trend. It was thus speculated that the higher aromaticity degree of the CHOS group in biomass smokes was attributed to the intensity variation of these simultaneously detected compounds, rather than the unique emission from a special source for the WIOC extract.

To explore the potential influence of fuel properties and combustion conditions on chemical composition, the major factors such as fuel moisture, $V_{daf}$, and parameters reflecting combustion conditions including MCE, and EC/OC ratios were assessed. The linear correlation analysis was applied to estimate the effect of these factors on each molecular intensity (commonly detected ones) (Fig.S10 and S11). The aliphatic compounds (including lipids-like, aliphatic/peptides-like, and carbohydrates-like compounds) were negatively correlated with the fuel moisture and positively

451 correlated with $V_{daf}$ and EC/OC ratios. Fuel moisture has been recognized as an important factor
452 influencing pollutant formation, but the influence is usually very complicated. The observed
453 relationship between fuel water content and pollutant EFs varies largely among studies, which may
454 be attributed to factors such as different water contents, pollutant types, and interactions among
455 other influencing factors. Fuels with high moisture levels may have high emissions, as extra energy
456 is needed to vaporize water during the burning process; however, a decrease in combustion
457 temperatures under very high-water content conditions may slow the pollutant formation rate and
458 consequently lower emissions. Higher EC/OC ratios and larger MCE values tend to be associated
459 with stronger flaming conditions. The results suggested that the aliphatic compounds were apt to be
460 produced during the period of the flaming phase with higher combustion temperature. This result
461 could partially explain that aliphatic/peptides-like compounds would be apt to be produced in the
462 improved stove rather than the traditional stove. In comparison, the emissions of CRAMs-like
463 compounds which are the most abundant species were decreased with the increased MCE and
464 EC/OC values, indicating that CARMs-like compounds were generated under the smoking phase.
465 No significant correlations of aromatics, unsaturated hydrocarbons, and HOCs were observed with
466 these parameters, resulting from their small proportion in commonly detected molecules. It is worth
467 noting that there may be significant differences, even for the same fuel, in chemical composition
468 depending on other factors such as stove type and combustion conditions. The interactions among
469 these factors make it difficult to assess their influence. It was found that only around 50% of
470 identified molecules were overlapped emissions for pine wood combusted in the traditional stove
471 and in the improved stove, suggesting the importance of the stove used. A smaller fraction of 25-
472 30% molecules were observed compared to the pine wood emissions with coals combusted in the
473 same stove, which suggested that the influence of varied fuels on chemical composition could
474 surpass the differences caused by different stoves. Our previous studies have revealed that fuel type

was the most important factor influencing the MAE values (Zhang et al., 2021b) and BrC EFs (Zhang et al., 2021a). The present study highlighted the dominant effect of fuel type on the chemical composition of soluble OC, providing a theoretical basis for source appointment based on molecular composition. Moreover, the combustion conditions would have a significant effect on the molecular intensity, resulting in differences in MAE eventually as indicated in section 3.1.

### 3.5 The correlation of light absorption properties with molecular compositions

Here we specifically investigate the variability in optical characteristics among the different fuels attributed to their chemical compositions. No significant correlations were observed between the AAE values of soluble OC and the molecular composition, indicating that AAE could be influenced by many factors. The MAE may be influenced by the degree of oxidation and unsaturation degree (Mo et al., 2017) (Tang et al., 2020), however, there was no significant correlation found between the MAE values and O/C values in the present source samples, implying that the BrC light absorption ability might not be directly affected by its oxidation degree.

The $MAE_{365, WSOC}$ values were significantly positively correlated with the DBE values ($r=0.786$, $p<0.05$) and the MW values ($r=0.750$, $p<0.05$) (Fig. S12), indicating that unsaturation and MW played a crucial role in the light absorption capability of the source samples. In the above discussion, we have noticed that the CHOS group in biomass was characterized by a higher degree of aromaticity than coal smoke aerosol, while the CHO, CHON, and CHONS groups have a higher aromatic degree in the coal emissions. A significantly positive correlation ($r=0.714$, $p<0.05$) was observed between $MAE_{365, WSOC}$ values, and the condensed aromatics percentages from the CHOS group (Fig. 6), indicating that aromatics in the CHOS group contributed to the high light absorption ability of biomass smokes.

For the WIOC extract, no significant correlation was found between the $MAE_{365, WIOC}$ values

with MW or DBE values, which might be explained by much different chemical composition for insoluble compounds compared with soluble parts Although the coal combustion emitted much more aromatic compounds with higher DBE values for the WIOC, the MAE values were not significantly higher. The significantly positive correlation (r=0.929, $p$<0.05) between $MAE_{365, WIOC}$ values, and the CHOS condensed aromatics percentages confirmed the importance of CHOS aromatics in determining the light absorption capability from source samples. As mentioned in Section 3.4, the higher aromaticity degree of the CHOS group in biomass smoke was largely due to the intensity variation of these commonly detected compounds in all source samples. Further analysis revealed that $MAE_{365, WIOC}$ values were positively correlated (r=0.750, $p$<0.05) with the CHOS condensed aromatics fractions which were the fraction simultaneously detected in all samples. These results indicated that the light absorption capability of source aerosols may be due to the higher abundance of some CHOS aromatic compounds commonly emitted from both coal and biomass, rather than the unique tracers.

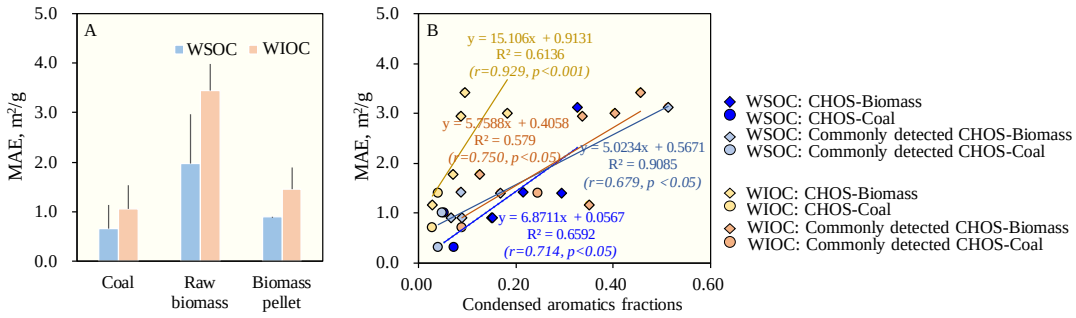


**Fig. 6** MAE values at λ=365 nm (A) and correlations between MAE values and condensed aromatics fractions in CHOS and in commonly detected CHOS (B) from the source samples

## 4. Conclusion and implication

The $MAE_{365, WSOC}$ ranged from 0.21 to 3.1 $m^2/g$ with an average of 1.3±0.7 $m^2/g$. The $MAE_{365, WIOC}$ was found to be higher with an average of 2.0±1.3 $m^2/g$. There were significant differences ($p$<0.05) observed among the different fuels for both $MAE_{365, WSOC}$ and $MAE_{365, WIOC}$, as raw

biomass burning combustion had significantly higher values than the coal combustion. The $AAE_{WSOC}$ ranged from 3.8 to 11 with an average of 6.9±1.5. The $AAE_{WIOC}$ was slightly lower than $AAE_{WSOC}$, which ranged from 4.2 to 6.5 with an average of 5.5±0.5. Thousands of peaks were identified in the m/z range of 150-800, indicating a complex chemical composition of aerosols from residential sources. CHO group was the most abundant component in the WSOC extracts and the contribution of CHO compounds to the total intensity in aerosols from raw biomass burning was significantly higher than those from biomass pellets and coal smoke. On the other hand, WIOC extract contained more SOCs, especially in the coal combustion aerosol. Notably, CHON compounds were more abundant in the coal combustion emissions, which was due to the higher fuel N content of coals ($r=0.936$, $p<0.05$). The SOCs emissions were more predominant during flaming phases, with a positive correlation between SOCs abundance with the MCE values ($r=0.750$, $p<0.05$). The CHO, CHON, and CHONS groups generated from coal combustion were characterized by high unsaturated levels with more aromatic species, while CHOS groups had higher aromaticity degrees in biomass smoke aerosols. It was found that MAE values were positively correlated with the CHOS condensed aromatics proportion for both WSOC ($r=0.714$, $p<0.05$) and WIOC extract ($r=0.929$, $p<0.001$). These results indicated that higher CHOS condense aromatics abundance in biomass burning aerosols could partly explain the higher MAE values of raw biomass smoke. Further analysis showed a positive correlation of MAE with the CHOS condensed aromatics fractions which were the fractions simultaneously detected in all samples. These results indicated that the light absorption capability of source aerosols may be due to the higher abundance of some CHOS aromatic compounds commonly emitted from both coal and biomass burning, rather than the unique tracers. The unique formulas of coal combustion aerosols were in the lower H/C and O/C regions with higher unsaturated compounds in the VK diagram. This work is potentially applicable to the source appointment based on the molecular characteristics and

to future studies developing more scientific control measures by focusing on one major component (e.g., CHOS condensed aromatics) of light absorption aerosols.

There are still some questions that need to be investigated in the future study. First, the study on BrC composition in this research used dissolved OC as a substitute. However, this substitute cannot fully represent BrC emissions. Both WSOC and WIOC contain some non-light-absorbing components, and the proportion of these components is unknown, making it difficult to measure the representativeness of extractable OC for BrC. Additionally, the lack of study about the emissions characteristics under controlled combustion conditions limits the obtained results. Controlled experiments including flaming or smoldering burns, airflow, and combustion temperature are needed in future work. Third, fresh burning-derived OC released into the atmosphere can undergo various aging reactions such as photochemical degradation. These reactions can significantly alter the light absorptivity and chemical properties of BrC components. It is essential to consider the optical properties and lifetimes of organic compounds emitted from solid fuel combustion in climate models.

**Data availability.**

Data are available by contacting the corresponding authors

**Supplement**

The following information is in the appendix and available via the Internet:

Data processing in the ESI FT-ICR MS; fuel properties of coal and biomass fuels tested; number of formulas in each group, values of elemental ratios, MW, and DBE values in the WSOC and WISCO for each source type; Stoichiometric ranges of VK classes; Correlation between fuel N and emission factors of NOx; the VK diagrams of WSOC and WIOC for different source samples;

and correlations between the VK plots of WSOC/WIOC and fuel properties or combustion conditions.

## Author contributions

LZ, GS, and ST designed the experiment. LZ and JL prepared the filters used. LZ, YL, XL and ZL conducted the sample collection. LZ and JL performed the data analysis. LZ wrote the paper. GS, and ST reviewed and commented on the paper.

## Competing interests

The authors declare that they have no conflict of interest.

## Acknowledgment

Funding for this study was partly from the National Natural Science Foundation of China (42077328, and 41922057). The authors greatly appreciated the valuable help in data analysis by Prof. Jianzhong Song from CAS.

## Financial support

This research has been supported by the National Natural Science Foundation of China (42077328, and 41922057)

## References

Bianco, A., Deguillaume, L., Vaitilingom, M., Nicol, E., Baray, J.L., Chaumerliac, N., and Bridoux, M.: Molecular Characterization of Cloud Water Samples Collected at the Puy de Dome (France) by Fourier Transform Ion Cyclotron Resonance Mass Spectrometry, Environ. Sci. Technol., 52, 10275-10285, https://doi.org/10.1021/acs.est.8b01964, 2018.

Bond, T. C.: Spectral dependence of visible light absorption by carbonaceous particles emitted from coal combustion, Geophys. Res. Lett., 28, 4075-4078, https://doi.org/10.1029/2001GL013652, 2001.

Bond, T. C. and Bergstrom, R. W.: Light absorption by carbonaceous particles: An investigative review, Aerosol Sci. Technol., 40, 27-67, https://doi.org/10.1080/02786820500421521, 2006.

Brege, M., Paglione, M., Gilardoni, S., Decesari, S., Facchini, M. C., and Mazzoleni, L. R.: Molecular insights on aging and aqueous-phase processing from ambient biomass burning

emissions-influenced Po Valley fog and aerosol, Atmos. Chem. Phys., 18, 13197-13214, https://doi.org/10.5194/acp-18-13197-2018, 2018.

Burling, I. R., Yokelson, R. J., Griffith, D. W. T., Johnson, T. J., Veres, P., Roberts, J. M., Warneke, C., Urbanski, S. P., Reardon, J., Weise, D. R., Hao, W. M., and de Gouw, J.: Laboratory measurements of trace gas emissions from biomass burning of fuel types from the southeastern and southwestern United States, Atmos. Chem. Phys., 10, https://doi.org/10.5194/acp-10-11115-2010, 2010.

Cao, T., Li, M., Zou, C., Fan, X., Song, J., Jia, W., Yu, C., Yu, Z., and Peng, P.: Chemical composition, optical properties, and oxidative potential of water- and methanol-soluble organic compounds emitted from the combustion of biomass materials and coal, Atmos. Chem. Phys., 21, 13187-13205, https://doi.org/10.5194/acp-21-13187-2021, 2021.

Chen, Y. and Bond, T. C.: Light absorption by organic carbon from wood combustion, Atmos. Chem. Phys., 10, 1773-1787, https://doi.org/10.5194/acp-10-1773-2010, 2010.

Du, Z., He, K., Cheng, Y., Duan, F., Ma, Y., Liu, J., Zhang, X., Zheng, M., and Weber, R.: A yearlong study of water-soluble organic carbon in Beijing II: Light absorption properties, Atmos. Environ., 89, 235-241, https://doi.org/10.1016/j.atmosenv.2014.02.022, 2014.

Fan, X., Li, M., Cao, T., Cheng, C., Li, F., Xie, Y., Wei, S., Song, J., and Peng, P. a.: Optical properties and oxidative potential of water-and alkaline-soluble brown carbon in smoke particles emitted from laboratory simulated biomass burning, Atmos. Environ., 194, 48-57, https://doi.org/10.1016/j.atmosenv.2018.09.025, 2018.

Feng, Y., Ramanathan, V., and Kotamarthi, V. R.: Brown carbon: a significant atmospheric absorber of solar radiation? Atmos. Chem. Phys., 13, 8607-8621, https://doi.org/10.5194/acp-13-8607-2013, 2013.

Hansson, K. M., Samuelsson, J., Tullin, C., and Amand, L. E.: Formation of HNCO, HCN, and NH3 from the pyrolysis of bark and nitrogen-containing model compounds, Combust. Flame, 137, 265-277, https://doi.org/10.1016/j.combustflame.2004.01.005, 2004.

He, T., Wu, Y., Wang, D., Cai, J., Song, J., Yu, Z., Zeng, X., and Peng, P. a.: Molecular compositions and optical properties of water-soluble brown carbon during the autumn and winter in Guangzhou, China, Atmos. Environ., 296, https://doi.org/10.1016/j.atmosenv.2022.119573, 2023.

Holder, A. L., Hagler, G. S. W., Aurell, J., Hays, M. D., and Gullett, B. K.: Particulate matter and black carbon optical properties and emission factors from prescribed fires in the southeastern United States, J. Geophys. Res.: Atmos., 121, 3465-3483, https://doi.org/10.1002/2015JD024321, 2016.

Huang, R.J., Yang, L., Cao, J., Chen, Y., Chen, Q., Li, Y., Duan, J., Zhu, C., Dai, W., Wang, K., Lin, C., Ni, H., Corbin, J. C., Wu, Y., Zhang, R., Tie, X., Hoffmann, T., O'Dowd, C., and Dusek, U.: Brown Carbon Aerosol in Urban Xi'an, Northwest China: The Composition and Light Absorption Properties, Environ. Sci. Technol., 52, 6825-6833, https://doi.org/10.1021/acs.est.8b02386, 2018.

Huang, R.J., Yang, L., Shen, J., Yuan, W., Gong, Y., Guo, J., Cao, W., Duan, J., Ni, H., Zhu, C., Dai, W., Li, Y., Chen, Y., Chen, Q., Wu, Y., Zhang, R., Dusek, U., O'Dowd, C., and Hoffmann, T.: Water-Insoluble Organics Dominate Brown Carbon in Wintertime Urban Aerosol of China: Chemical Characteristics and Optical Properties, Environ. Sci. Technol., 54, 7836-7847, https://doi.org/10.1021/acs.est.0c01149, 2020.

Huo, Y., Li, M., Jiang, M., and Qi, W.: Light absorption properties of HULIS in primary particulate matter produced by crop straw combustion under different moisture contents and stacking modes, Atmos. Environ., 191, 490-499, https://doi.org/10.1016/j.atmosenv.2018.08.038, 2018.

Jen, C. N., Hatch, L. E., Selimovic, V., Yokelson, R. J., Weber, R., Fernandez, A. E., Kreisberg, N. M., Barsanti, K. C., and Goldstein, A. H.: Speciated and total emission factors of particulate

organics from burning western US wildland fuels and their dependence on combustion efficiency, Atmos. Chem. Phys., 19, 1013-1026, https://doi.org/10.5194/acp-19-1013-2019, 2019.

Jiang, B., Kuang, B. Y., Liang, Y., Zhang, J., Huang, X. H. H., Xu, C., Yu, J. Z., and Shi, Q.: Molecular composition of urban organic aerosols on clear and hazy days in Beijing: a comparative study using FT-ICR MS, Environ. Chem., 13, 888-901, https://doi.org/10.1071/EN15230, 2016.

Jiang, H., Li, J., Sun, R., Tian, C., Tang, J., Jiang, B., Liao, Y., Chen, C.-E., and Zhang, G.: Molecular Dynamics and Light Absorption Properties of Atmospheric Dissolved Organic Matter, Environ. Sci. Technol., 55, 10268-10279, https://doi.org/10.1021/acs.est.1c01770, 2021.

Jo, D. S., Park, R. J., Lee, S., Kim, S.-W., and Zhang, X.: A global simulation of brown carbon: implications for photochemistry and direct radiative effect, Atmos. Chem. Phys., 16, 3413-3432, https://doi.org/10.5194/acp-16-3413-2016, 2016.

Laskin, A., Laskin, J., and Nizkorodov, S. A.: Chemistry of Atmospheric Brown Carbon, Chem. Rev., 115, 4335-4382, https://doi.org/10.1021/cr5006167, 2015.

Laskin, A., Smith, J. S., and Laskin, J.: Molecular Characterization of Nitrogen-Containing Organic Compounds in Biomass Burning Aerosols Using High-Resolution Mass Spectrometry, Environ. Sci. Technol., 43, 3764-3771, https://doi.org/10.1021/es803456n, 2009.

Li, J., Zhang, Q., Wang, G., Li, J., Wu, C., Liu, L., Wang, J., Jiang, W., Li, L., Ho, K. F., and Cao, J.: Optical properties and molecular compositions of water-soluble and water-insoluble brown carbon (BrC) aerosols in northwest China, Atmos. Chem. Phys., 20, 4889-4904, https://doi.org/10.5194/acp-20-4889-2020, 2020.

Li, M., Fan, X., Zhu, M., Zou, C., Song, J., Wei, S., Jia, W., and Peng, P. a.: Abundance and Light Absorption Properties of Brown Carbon Emitted from Residential Coal Combustion in China, Environ. Sci. Technol., 53, 595-603, https://doi.org/10.1021/acs.est.8b05630, 2019.

Lin, P., Rincon, A. G., Kalberer, M., and Yu, J. Z.: Elemental Composition of HULIS in the Pearl River Delta Region, China: Results Inferred from Positive and Negative Electrospray High Resolution Mass Spectrometric Data, Environ. Sci. Technol., 46, 7454-7462, https://doi.org/10.1021/es300285d, 2012.

Lv, J., Zhang, S., Wang, S., Luo, L., Cao, D., and Christie, P.: Molecular-Scale Investigation with ESI-FT-ICR-MS on Fractionation of Dissolved Organic Matter Induced by Adsorption on Iron Oxyhydroxides, Environ. Sci. Technol., 50, 2328-2336, https://doi.org/10.1021/acs.est.5b04996, 2016.

McMeeking, G. R., Kreidenweis, S. M., Baker, S., Carrico, C. M., Chow, J. C., Collett, J. L., Jr., Hao, W. M., Holden, A. S., Kirchstetter, T. W., Malm, W. C., Moosmueller, H., Sullivan, A. P., and Wold, C. E.: Emissions of trace gases and aerosols during the open combustion of biomass in the laboratory, J. Geophys. Res.: Atmos., 114, https://doi.org/10.1029/2009JD011836, 2009.

Mo, Y., Li, J., Liu, J., Zhong, G., Cheng, Z., Tian, C., Chen, Y., and Zhang, G.: The influence of solvent and pH on determination of the light absorption properties of water-soluble brown carbon, Atmos. Environ., 161, 90-98, https://doi.org/10.1016/j.atmosenv.2017.04.037, 2017.

Mo, Y., Zhong, G., Li, J., Liu, X., Jiang, H., Tang, J., Jiang, B., Liao, Y., Cheng, Z., and Zhang, G.: The Sources, Molecular Compositions, and Light Absorption Properties of Water-Soluble Organic Carbon in Marine Aerosols From South China Sea to the Eastern Indian Ocean, J. Geophys. Res.: Atmos., 127, https://doi.org/10.1029/2021JD036168, 2022.

Olson, M. R., Garcia, M. V., Robinson, M. A., Van Rooy, P., Dietenberger, M. A., Bergin, M., and Schauer, J. J.: Investigation of black and brown carbon multiple-wavelength-dependent light absorption from biomass and fossil fuel combustion source emissions, J. Geophys. Res.: Atmos., 120, 6682-6697, https://doi.org/10.1002/2014JD022970, 2015.

Park, S. S. and Yu, J.: Chemical and light absorption properties of humic-like substances from

685 biomass burning emissions under controlled combustion experiments, Atmos. Environ., 136, 114-
686 122, https://doi.org/10.1016/j.atmosenv.2016.04.022, 2016.

687 Patriarca, C., Bergquist, J., Sjoberg, P. J. R., Tranvik, L., and Hawkes, J. A.: Online HPLC-
688 ESI-HRMS Method for the Analysis and Comparison of Different Dissolved Organic Matter
689 Samples, Environ. Sci. Technol., 52, 2091-2099, https://doi.org/10.1021/acs.est.7b04508, 2018.

690 Pokhrel, R. P., Wagner, N. L., Langridge, J. M., Lack, D. A., Jayarathne, T., Stone, E. A.,
691 Stockwell, C. E., Yokelson, R. J., and Murphy, S. M.: Parameterization of single-scattering albedo
692 (SSA) and absorption Angstrom exponent (AAE) with EC / OC for aerosol emissions from biomass
693 burning, Atmos. Chem. Phys., 16, 9549-9561, 10.5194/acp-16-9549-2016, 2016.

694 Rathod, T., Sahu, S. K., Tiwari, M., Yousaf, A., Bhangare, R. C., and Pandit, G. G.: Light
695 Absorbing Properties of Brown Carbon Generated from Pyrolytic Combustion of Household
696 Biofuels, Aerosol Air Qual. Res., 17, 108-116, 10.4209/aaqr.2015.11.0639, 2017.

697 Reisen, F., Meyer, C. P., Weston, C. J., and Volkova, L.: Ground-Based Field Measurements of
698 PM2.5 Emission Factors From Flaming and Smoldering Combustion in Eucalypt Forests, J.
699 Geophys. Res.: Atmos., 123, 8301-8314, https://doi.org/10.1029/2018JD028488, 2018.

700 Ren, Q. and Zhao, C.: Evolution of fuel-N in gas phase during biomass pyrolysis, Renewable
701 Sustainable Energy Rev., 50, 408-418, https://doi.org/10.1016/j.rser.2015.05.043, 2015.

702 Saleh, R., Robinson, E. S., Tkacik, D. S., Ahern, A. T., Liu, S., Aiken, A. C., Sullivan, R. C.,
703 Presto, A. A., Dubey, M. K., Yokelson, R. J., Donahue, N. M., and Robinson, A. L.: Brownness of
704 organics in aerosols from biomass burning linked to their black carbon content, Nat. Geosci., 7, 647-
705 650, 10.1038/ngeo2220, 2014.

706 Song, J., Li, M., Jiang, B., Wei, S., Fan, X., and Peng, P. a.: Molecular Characterization of
707 Water-Soluble Humic like Substances in Smoke Particles Emitted from Combustion of Biomass
708 Materials and Coal Using Ultrahigh-Resolution Electrospray Ionization Fourier Transform Ion
709 Cyclotron Resonance Mass Spectrometry, Environ. Sci. Technol., 52, 2575-2585,
710 https://doi.org/10.1021/acs.est.7b06126, 2018.

711 Song, J., Li, M., Fan, X., Zou, C., Zhu, M., Jiang, B., Yu, Z., Jia, W., Liao, Y., and Peng, P. a.:
712 Molecular Characterization of Water- and Methanol-Soluble Organic Compounds Emitted from
713 Residential Coal Combustion Using Ultrahigh-Resolution Electrospray Ionization Fourier
714 Transform Ion Cyclotron Resonance Mass Spectrometry, Environ. Sci. Technol., 53, 13607-13617,
715 https://doi.org/10.1021/acs.est.9b04331, 2019.

716 Sun, J. Z., Zhi, G. R., Hitzenberger, R., Chen, Y. J., Tian, C. G., Zhang, Y. Y., Feng, Y. L.,
717 Cheng, M. M., Zhang, Y. Z., Cai, J., Chen, F., Qiu, Y., Jiang, Z., Li, J., Zhang, G., and Mo, Y.:
718 Emission factors and light absorption properties of brown carbon from household coal combustion
719 in China, Atmos. Chem. Phys., 17, 4769-4780, https://doi.org/10.5194/acp-17-4769-2017, 2017.

720 Tang, J., Li, J., Su, T., Han, Y., Mo, Y., Jiang, H., Cui, M., Jiang, B., Chen, Y., Tang, J., Song,
721 J., Peng, P. a., and Zhang, G.: Molecular compositions and optical properties of dissolved brown
722 carbon in biomass burning, coal combustion, and vehicle emission aerosols illuminated by
723 excitation-emission matrix spectroscopy and Fourier transform ion cyclotron resonance mass
724 spectrometry analysis, Atmos. Chem. Phys., 20, 2513-2532, https://doi.org/10.5194/acp-20-2513-
725 2020, 2020.

726 Wang, Q. Q., Zhou, Y. Y., Ma, N., Zhu, Y., Zhao, X. C., Zhu, S. W., Tao, J. C., Hong, J., Wu,
727 W. J., Cheng, Y. F., and Su, H.: Review of Brown Carbon Aerosols in China: Pollution Level, Optical
728 Properties, and Emissions, J. Geophys. Res.: Atmos., 127, https://doi.org/10.1029/2021JD035473,
729 2022.

730 Wei, W., Xie, Q., Yan, Q., Hu, W., Chen, S., Su, S., Zhang, D., Wu, L., Huang, S., Zhong, S.,
731 Deng, J., Yang, T., Li, J., Pan, X., Wang, Z., Sun, Y., Kong, S., and Fu, P.: Dwindling aromatic
732 compounds in fine aerosols from chunk coal to honeycomb briquette combustion, Sci. Total

Environ., 838, https://doi.org/10.1016/j.scitotenv.2022.155971, 2022.

Wozniak, A. S., Bauer, J. E., Sleighter, R. L., Dickhut, R. M., and Hatcher, P. G.: Technical Note: Molecular characterization of aerosol-derived water soluble organic carbon using ultrahigh resolution electrospray ionization Fourier transform ion cyclotron resonance mass spectrometry, Atmos. Chem. Phys., 8, 5099-5111, https://doi.org/10.5194/acp-8-5099-2008, 2008.

Xie, M. J., Hays, M. D., and Holder, A. L.: Light-absorbing organic carbon from prescribed and laboratory biomass burning and gasoline vehicle emissions, Sci. Rep., 7, https://doi.org/10.1038/s41598-017-06981-8, 2017.

Xiong, R., Li, J., Zhang, Y., Zhang, L., Jiang, K., Zheng, H., Kong, S., Shen, H., Cheng, H., Shen, G., and Tao, S.: Global brown carbon emissions from combustion sources, Environ. Sci. Ecotechnology, 12, 100201, https://doi.org/10.1016/j.ese.2022.100201, 2022.

Yokelson, R. J., Susott, R., Ward, D. E., Reardon, J., and Griffith, D. W. T.: Emissions from smoldering combustion of biomass measured by open-path Fourier transform infrared spectroscopy, J. Geophys. Res.: Atmos.,, 102, 18865-18877, 10.1029/97jd00852, 1997.

Yue, S., Zhu, J., Chen, S., Xie, Q., Li, W., Li, L., Ren, H., Su, S., Li, P., Ma, H., Fan, Y., Cheng, B., Wu, L., Deng, J., Hu, W., Ren, L., Wei, L., Zhao, W., Tian, Y., Pan, X., Sun, Y., Wang, Z., Wu, F., Liu, C.-Q., Su, H., Penner, J. E., Poschl, U., Andreae, M. O., Cheng, Y., and Fu, P.: Brown carbon from biomass burning imposes strong circum-Arctic warming, One Earth, 5, 293-304, https://doi.org/10.1016/j.oneear.2022.02.006, 2022.

Zhang, L., Luo, Z., Du, W., Li, G., Shen, G., Cheng, H., and Tao, S.: Light absorption properties and absorption emission factors for indoor biomass burning, Environ. Pollut., 267, https://doi.org/10.1016/j.envpol.2020.115652, 2020.

Zhang, L., Luo, Z. H., Li, Y. J., Chen, Y. C., Du, W., Li, G., Cheng, H. F., Shen, G. F., and Tao, S.: Optically Measured Black and Particulate Brown Carbon Emission Factors from Real-World Residential Combustion Predominantly Affected by Fuel Differences, Environ. Sci. Technol., 55, 169-178, https://doi.org/10.1021/acs.est.0c04784, 2021a.

Zhang, L., Luo, Z., Xiong, R., Liu, X., Li, Y., Du, W., Chen, Y., Pan, B., Cheng, H., Shen, G., and Tao, S.: Mass Absorption Efficiency of Black Carbon from Residential Solid Fuel Combustion and Its Association with Carbonaceous Fractions, Environ. Sci. Technol., 55, 10662-10671, https://doi.org/10.1021/acs.est.1c02689, 2021b.

Zhang, L., Hu, B., Liu, X., Luo, Z., Xing, R., Li, Y., Xiong, R., Li, G., Cheng, H., Lu, Q., Shen, G., and Tao, S.: Variabilities in Primary N-Containing Aromatic Compound Emissions from Residential Solid Fuel Combustion and Implications for Source Tracers, Environ. Sci. Technol., https://doi.org/10.1021/acs.est.2c03000, 2022.

Zhao, Y., Hallar, A. G., and Mazzoleni, L. R.: Atmospheric organic matter in clouds: exact masses and molecular formula identification using ultrahigh-resolution FT-ICR mass spectrometry, Atmos. Chem. Phys., 13, 12343-12362, https://doi.org/10.5194/acp-13-12343-2013, 2013.